

# Characterization of Vulnerability of Road Networks to Fluvial Flooding using SIS Network Diffusion Model

Bahrulla Abdulla; Amin Kiaghadi; Hannadi S. Rifai; Bjorn Birgisson

## ABSTRACT

This study aims to characterize the vulnerability of road networks to fluvial flooding using a network diffusion-based method. Various network diffusion models have been applied widely for modeling the spreading of contagious diseases or capturing the opinion dynamics in social networks. By comparison, their application in the context of physical infrastructure networks has just started to gain some momentum, although physical infrastructure networks also exhibit diffusion-like phenomena under certain stressors. This study applies a susceptible-impacted-susceptible (SIS) diffusion model to capture the impact of the fluvial flooding on the road network connectivity. To that end, this paper undertakes the following four steps. First, we modeled the road network as primal graphs and identified nodes that are flood-prone (or the origins of the fluvial flood). Second, temporal changes in the flood depth within the road network during a flooding event were obtained using hydraulic models. Third, based on the relationship between vehicle speed and flood depth on road networks, at each time step, the nodes in the road network were divided into two discrete categories, namely functional and closed, standing for Susceptible and Impacted in the SIS diffusion model, respectively. Then, two parameters of the SIS model, average transition probabilities between states, were estimated using the results of the hydraulic simulation. Fourth, the robustness of the road network under various SIS diffusion scenarios was estimated, which was used to test the statistical significance of the difference between the robustness of the road network against diffusions started from the randomly chosen nodes and nodes with high centrality measures. The methodology mentioned above was demonstrated using the road network in the Memorial Super neighborhood in Houston. The results show that a diffusive disruption which starts from nodes with high centrality values does not necessarily cause more significant loss to the connectivity of the road network. The proposed method has important implications for applying link predictions on road networks, and it casts significant insights into the mechanism by which cascading disruptions spread from flood control infrastructure to the road networks, as well as the diffusion process in the road networks.

**Keywords:** Road Network; Fluvial Flooding; SIS Diffusion; Network Vulnerability; Giant Connected Component (GCC); Diffusion Patterns; Network Centrality Measures

## I. INTRODUCTION

Changes in the earth climate, potential global warming, and unprecedented and ever-increasing urbanization, coupled with the increased interdependence among different sectors, are putting the critical infrastructure systems under increasing pressure (Rodin, 2014). In the meantime, failures in critical infrastructure systems are becoming prohibitively costly, mainly due to the possible cascading failures that are initiated from one sector and subsequently cause a series of failures in other dependent sectors. Thus, the resilience of interdependent critical infrastructure (ICI) systems is one of the grand challenges facing engineers and policy-makers in the 21<sup>st</sup> century (Heller, 2002; O'Rourke, 2007; van Laere et al., 2017). Over the past two decades, the body of knowledge on ICI resilience has advanced in the domains of modeling, simulation methods, and theoretical frameworks. Despite the growing literature (Dueñas-Osorio, Craig, Goodno, & Bostrom, 2007; Haimes & Jiang, 2001; Reed, Kapur, & Christie, 2009) on ICI resilience, our understanding of the dynamics and mechanisms of disruptions in ICI systems that shape resilience patterns in these complex networks is somewhat limited. This is particularly evident in urban areas where transport systems are frequently affected by weather-related hazards.

Flooding, especially ones due to excessive and intense rainfall precipitation, has been the predominant cause of the weather-related disruptions to the transportation infrastructure (Pregnolato, Ford, Wilkinson, & Dawson, 2017). Such events could undermine the vital functionality of transportation systems, especially road networks. Many studies have shown that roads are among the major causes of deaths in cities during flooding; this is mainly due to the vehicles being driven through flooded roadways (Ashley & Ashley, 2008; Drobot, Benight, & Grunfest, 2007; FitzGerald, Du, Jamal, Clark, & Hou, 2010; Kreibich et al., 2009). Locations, such as Texas, where road mobility through cars is the primary mode of passenger transportation, are especially vulnerable to the impact of flooding (Blackburn, 2017), as the advantage of having the largest road networks in the U.S. could become a curse when the majority of the road networks are closed due to flooding events and there are few other alternatives to go around the city, as was the case during Hurricane Harvey in 2017 (ASCE, 2017). In addition, during the disastrous events, the road system functions as a lifeline system for rescuing people and assets and plays a

vital role in repairing and restoring other infrastructure systems when they are disrupted. In order to cope with disruptions efficiently and take active precautionary measures, it is critical to understand the mechanisms and patterns with which the disruptions unfold in the transportation network. Due to the planar nature of transportation networks, they tend to lend themselves readily to being represented as graphs, and therefore graph theory-based approaches have been one of the standard tools to study the vulnerability in the transportation systems (Tamvakis & Xenidis, 2013). Graph theory reduces a road network to a mathematical matrix where the vertices (nodes) represent road intersections and the edges are the road sections between these nodes (Leu, Abbass, & Curtis, 2010). This type of matrix abstraction of road networks not only facilitates the accessibility and connectivity analysis but also assists in the identification of critical locations using available graph-theoretic centrality measures. However, there are two crucial challenges in network modeling of transportation networks. On the one hand, transportation networks, like many other critical infrastructure networks, are spatially embedded (Bashan, Berezin, Buldyrev, & Havlin, 2013) and the configurations of the environment in which network elements (nodes or edges) operates are inherently heterogeneous, which, coupled with the possible spatial or temporal variance of the magnitude of the disruptive events, makes failure probabilities vary significantly from node to node. On the other hand, the topology of most critical infrastructure networks is intrinsically dynamic and evolving, especially during disruptive events. While an understanding of the patterns for temporal shifts in the functional topology of the critical infrastructure networks during disastrous events remains a crucial step in devising efficient plans to reduce their vulnerabilities, the almost complete absence of the time dimension in such problem definitions can be attributed to: (1) the graph theory ancestry of the field, and in (2) the limited number of dynamic data sources available when the area of complex networks analysis emerged (Rossetti et al., 2018).

Flooding in urban roadways is a process that presents both of the challenges mentioned above. Relevant studies in the literature that aimed at tackling the flood vulnerability of critical infrastructure networks could be categorized into two main types: (1) graph-theory based topological approaches that focus on topological integrity of the network; (2) hydrological approaches that models the flood

propagation process in (or around) critical infrastructure in urban areas (Singh, Sinha, Vighani, & Pahuja, 2018). Each of these methods tackles the flood vulnerability problem from different angles; consequently, it only paints some parts of the whole picture. Most of the studies which attempted to apply dynamic network modeling approaches focused on complete or random graphs to demonstrate its applicability in real-world network failure problems. However, transportation networks are neither random nor complete. They have a unique configuration manifested in a relatively small range of node-degrees and spatial constraints which is not observed in other types of networks. This historical decoupling between two types of methods could largely be attributed to the lack of granular flood data which could be inputted to the network modeling.

Recently, for identifying the probability of flooding in a road network, the coupling of remotely sensed data with hydrodynamic models has been used. Such an approach was used to identify the most critical and vulnerable nodes (intersections) in a transportation network. Sadler et al. (2017) combined storm surge levels associated with different return periods, provided by the Federal Emergency Management Administration (FEMA), with High-resolution Digital Elevation Models (DEMs), compiled from data collected by Light Detection and Ranging (LiDAR). The authors then compared the surge elevations with the road elevations to assess different scenarios and reported the most vulnerable roadway segments based on the frequency of flooding. In another study, Kalantari et al. (2017) developed a LiDAR-based data-driven model to quantify the risk of flooding and sediment transport at different roadway intersections in Sweden. While these efforts are essential to study the impacts of the most severe inundation scenarios, they do not provide enough information on how the internal components of the system behave during a flood event. This restriction is mainly due to the use of only one snapshot of the flood rather than a time series of water depth. In contrast, other researchers have coupled the results of hydrodynamic models to estimate the probability of flooding during the flooding events. Courty et al. (2017), Lagmay et al. (2017), and Pyatkova et al. (2019) coupled the results of MIKE FLOOD, LISFLOOD-FP, and FLO-2D GDS PRO, respectively, to LiDAR elevations and reported the risk of inundation for roads during flooding events. Though more accurate hydrodynamic models are useful tools

in storm surge and flood simulation/prediction, they are expensive to apply because of lengthy computational time, expensive equipment and the need for skilled users. In addition, an extensive calibration of the model using observed data is required to make the model results reliable. In summary, existing methods are either focused on a single point in the duration of the disastrous event and there is a lack of understanding about the internal mechanism of the disruptive events on road networks; or are computationally or operationally too expensive. This study aims to bridge the gaps mentioned above between these two closely related fields. Furthermore, given the improved computational powers and relatively wide availability of the data, the condition is mature enough to do a more granular and detailed temporal analysis on the road network. This study is motivated as such. In this study, a simple methodology was developed to have both the reliability of using the field measured data directly and the advantage of using time series water depth instead of one snapshot. To be more specific, the measured high-water marks (HWMs) after a flooding event were combined with the observed pattern in water surface elevation (WSE) of nearby rivers recorded by USGS to create a WSE time series at the location of the HWMs. Each time series was then compared with LiDAR elevations to calculate the water depth at any given point.

When it comes to analyzing the effect of flooding on network vulnerability, it is important to know how a phenomenon spreads through a network. Based on authors' interview with stakeholders of critical infrastructure systems in Houston, after flood control infrastructures (Bayous, channels, creeks, and stormwater systems) reached their capacity under an excessive rainfall, road networks become part of the flood control infrastructure and play the role of conducting excessive water into lower elevation areas or releasing into storm-water drainage systems. In this context, the process of spreading the floodwater around the road network could be assumed as a diffusion process, which is analogous to the spread of contagious diseases among human beings. The origin of the diffusion modeling could be traced back to the spread of epidemics and mathematical modeling of epidemics predates most of the studies on networks by many years (Newman, 2010). The traditional diffusion modeling approaches avoid discussing contact networks by making use of fully mixed or mass-action approximation, in which it is

assumed that every individual (node in the network) has an equal chance, per unit of time, of coming into contact with every other (Newman, 2018). According to the assumptions of this approach, nodes (people) mingle and meet completely at random, which is not a realistic representation of any real-world networks. This is because nodes in real-world networks are spatially embedded and have a heterogeneous exposure to diffusion mechanisms. Shakarian et al. (2015) have provided a comprehensive review of the papers and recent research work in the field of network diffusion.

In conclusion, the majority of the research in the field of network vulnerability is focused on theoretical networks; relatively, a fewer number of published research papers are focused on real-world networks. Due to their unique topological structure and the configuration, road networks represent one unique type of real-world networks. Understanding, characterizing, and theorizing these networks could bridge the gap between advancement in the field of theoretical networks and real-world networks. The proposed method facilitates the assessment of the vulnerability of the road network which contributes to the advancement of network science in the realm of real-life networks. This is because this type of flooding happens all around the globe, the findings from this research are directly applicable to other road networks.

## II. METHODOLOGY

A summary of the methodology followed in this study is presented in Figure 1. The first step was modeling the road systems as the primal graph, which is followed by a simulation of the hydraulic process in the areas where roads located in order to obtain the granular (node-level) flood depth data. A diffusion model that commonly used to study the spread of communicable disease, Susceptible-Impacted-Susceptible (SIS Model), is proposed to model the propagation of the flood in road networks. Parameters of the SIS model were estimated using the temporal flood depth for the nodes in the road network. Finally, the impact of both the number and locations of the seed nodes on the connectivity of the road networks during diffusion were evaluated.

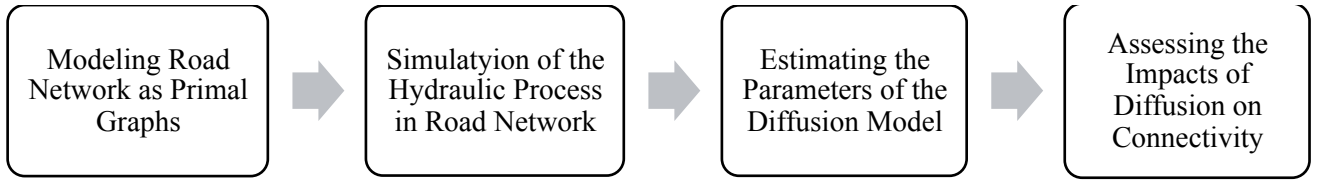


**Figure 1 Research Methodology**

### 1. Road Network Modelling

The road network was modeled as a non-planar primal graph, where nodes represent the intersections in the road network while edges represent the actual road sections. As a proxy for the flood vulnerability, the elevation of each node in the network was also retrieved using Google API. Road network topological data and other auxiliary information were obtained from OpenStreetMap using the OSMnx python package (Boeing, 2017).

### 2. Simulation of the Hydraulic Process

In this study, the depth of flooding at nodes of the road network was used as a proxy for their functional status. Therefore, obtaining the granular temporal flood depth information in the road network during the case study event— Hurricane Harvey, was crucial. During Harvey, flooding in the study started at 20:00:00 on August 26, 2017. The temporal changes in the flood depth at the node location in the road network is obtained for a temporal scale of 17 days, observations are in hourly intervals, from 12 AM, 25 August 2017 to 11 PM, 10 September 2017. This study looked into the time between 22:00:00 on August 26, 2017, and above peak period, which is 11:00:00 on August 30, 2017.

The methodology applied in this study to calculate the water depth at each node of the road network is similar to what Kiaghadi et al. (2019) developed. The main difference was converting the observed HWMs (one snapshot of the flood representing the maximum WSE) into a time series. In other words, in this study, a water surface elevation over the time of the flooding event (i.e. Hurricane Harvey) was used instead of a static snapshot of the event. Due to a smaller study area, all calculations were undertaken at the catchment level and only HWMs within the catchments covering the study area were used. Catchment boundaries were extracted from the watershed delineation in the Tropical Storm Allison

Recovery Project (TSARP). Figure 2 shows the catchments and associated HWMs used in this study. A total of 11 HWMs were used.

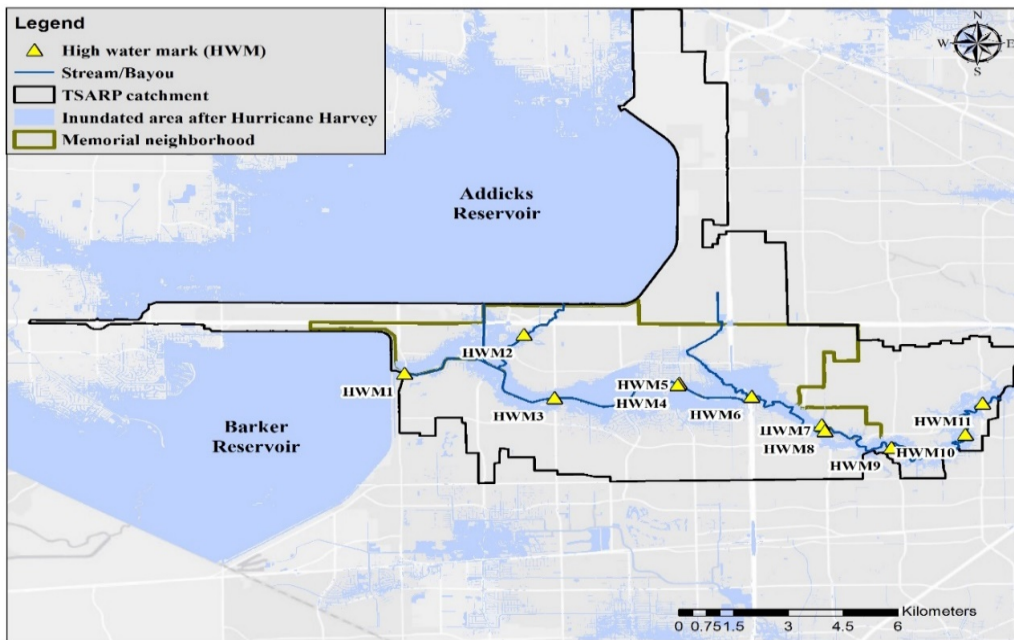


**Figure 2 Study area and location of High-Water Marks (HWMs) used in this study**

To convert the single measured HWM into a WSE time series, the observed pattern in the WSE at the closest USGS gage to the HWM location was used. Since the majority of the HWMs were measured close to the banks of rivers and were caused by the river over banking, it was assumed that the WSE time series at the location of the HWM was similar to the river behavior. The HWM represents the highest level of water observed at the specific location that is equivalent to the peak of the WSE time-series recorded by USGS. For the period of simulation and for each USGS gage, the ratio between the WSE at each time step and the peak were calculated and multiplied to the reported values of nearby HWMs to generate the WSE time series at the location of each HWM. For HWMs located on the tributaries (see HWM2 in Figure 2), the pattern observed in the difference between recorded discharges from two USGS gages (one upstream and one downstream) was applied to the HWMs. Here, it was assumed that the difference in the discharge rates was solely caused by the input from the tributary and not by the direct runoff from the drainage areas between the two USGS gages. To automate the process of generating a

WSE at each time step (one hour) a model was built in ArcMap. Several existing tools in ArcMap were applied to (1) Convert the HWMs within the catchments into a WSE raster with a resolution of 1 m by 1 m for each time step; (2) Subtract the surface elevation raster (LiDAR DEM) from the WSE raster to calculate the water depth at time steps; (3) Extract the water depths at the locations of specific nodes (intersections) for each time step; (4) Filter the depths to only consider nodes with a positive depth. A negative value indicates that the river water is contained within the original river bank; (5) Export the excel file containing the locations and associated water depths. In the end, A MATLAB code was also developed to combine all the excel files and create a metafile with the locations of the nodes and water depth at each time step over the length of the simulation.

### 3. Estimation of the Parameters of the SIS Network Diffusion Model

In this study, it was hypothesized that the propagation of the flooding impacts in the road network can be modeled using the SIS diffusion approach. In SIS diffusion, there are two types of nodes (Susceptible and Infected) and the rate of change between these two statuses are characterized by two parameters called beta and gamma (See Figure 3). The main reason to focus on the nodes, instead of links (which seemingly is more appropriate in the context of the road network) is because once a node is flooded enough to be removed from the network, the edges connected to that node will be rendered as nonfunctional

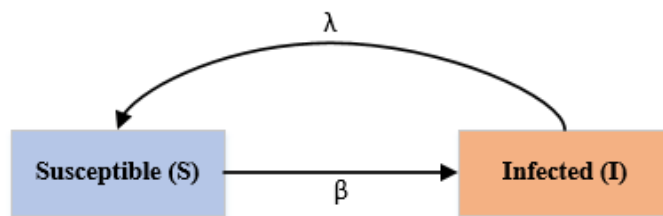


**Figure 3 Flowchart for the SIS Diffusion Model**

The first task in SIS diffusion modeling is to categorize the study population (nodes in this context) into different classes using certain criteria defined by the user. For this study, it is possible to categorize the nodes in the road network into functional or closed categories. During a flooding event,

the closed or functional status of the road network is a binary value, but the flooding (depth) status in different parts of the road network is a continuous variable. It is possible to relate the flood depth to closed or functional status of roads via vehicle speed. Researchers have studied the relationship between the depth of the flooding and the speed of the vehicles driving on the roads during the flooding event. Pregnolato et al. (2017) have estimated the relationship between the depth of standing water and the speed of different types of vehicles as:

$$v(w) = 0.0009w^2 - 0.5529w + 86.9448 \quad (1)$$

where:

$v(w)$  is the vehicle speed and  $w$  is the depth of the floodwater on the road.

Using the above Equation1, nodes in the road network at any given point in time are divided into two categories based on the vehicle speed. (1) **Susceptible Nodes (S):** The susceptible group is a node in the network which is either intact at a given point or flood depth in the node location is less than 140mm. On these types of nodes, the passenger vehicle speed is more than or equal to 20km/h. (2) **Infected Nodes (I):** The Impacted group is the nodes that have been heavily impacted by the flood and are rendered non-functional. The speed of vehicles on these types of nodes is less than 20km/h.

The next step in SIS diffusion modeling is to identify the seed nodes, the portion of the nodes in the network, which were already impacted when diffusion started. During a fluvial flooding event, the nodes located within the flood-prone areas initiate a flood-induced diffusion phenomenon in the road network. Estimating the flood-proneness of the nodes can be based on the floodplain type, proximity to flood control infrastructure and relative elevation of the nodes (Abdulla, Mostafavi, & Birgisson, 2019). The last step is to estimate the other two essential parameters of the SIS diffusion,  $\beta$  and  $\gamma$ . Parameters of the diffusion are solved using equations (2) and (3) provided by Newman (2018):

$$\frac{dS}{dt} = \gamma x - \beta sx \quad (2)$$

$$x(t) = x_0 \frac{(\beta - \gamma)e^{(\beta - \gamma)t}}{\beta - \gamma + \beta x_0 e^{(\beta - \gamma)t}} \quad (3)$$

where:

$\beta$  and  $\gamma$ : transition parameters of diffusion;  $S$ : number of Susceptible individuals (nodes) at a given point in time;  $I$ : number of Infected individuals (nodes) at a given point in time;  $x(t)$ : the fraction of infected nodes at a given point in time;  $x_0$ : the fraction of susceptible nodes at the beginning of diffusion.

Simulation of the SIS diffusion in the road network under hypothetical cascading failures was conducted using the NDlib python package (Rossetti et al., 2018).

#### **4. Assessing the Diffusion Profile and Connectivity under Different Scenarios**

Two impacts of the flood-induced network diffusion on the road network are studied. One is the impacts of the diffusion started at different locations on the connectivity profile of the road network. The other one is the impact of diffusion on the overall connectivity of the road network during the flood propagation process in the road network.

- **Connectivity Profile**

Due to diverse colocation patterns between road networks and flood control infrastructure networks, it is possible for the fluvial flooding to occur at any location in the road network. This scenario analysis estimated the impacts of the locations of nodes with specific centrality measures on the diffusion profile of the road networks using the relative (to original network size) size of the connected giant component (GCC) in the road network. Due to the unique topography and layout of the road networks, nodes with high centrality measures represent unique locations on the road networks. Five considered scenarios are: (1) diffusion is initiated from a certain number of randomly selected nodes; (2) diffusion started from a certain number of nodes with the highest betweenness centrality; (3) diffusion started from a certain number of nodes with highest degree centrality; (4) diffusion started from a certain number of nodes with highest closeness centrality; (5) diffusion started from a certain number of nodes with highest eigenvector centrality. For this analysis, the road network in the Memorial super neighborhood was used.

- **Overall Connectivity**

While connectivity profile could cast some insights into the sensitivity of the diffusion at different levels on the connectivity of the road network, it is not an aggregate measure of the overall impact of flooding on the road connectivity. Therefore, a measure called overall connectivity (OC) is introduced to assess the connectivity of the network during the diffusive disruptive events. The connectivity changes due to diffusive disruptions are quite uneven under different scenarios. In order to make the magnitude of the impacts of different diffusions on road network comparable, the area under the performance curve is calculated. OC is defined in below way (see Equation 4):

$$OC = \int_{t_0}^{t_1} GC(t) dt \quad (4)$$

where:

$t_0$  – the starting time for the disruptive event;

$t_1$  – the time the disruptive event ends;

$GC(t)$  – the relative size of the connected giant component in road network.

In order to examine the impacts of the location of the initial diffusive set seeds on the vulnerability of the road network, this study has conducted a two-sample significance test. The working hypothesis is road network is more vulnerable to the contagious disruptions which start from those significant nodes. Because removal of these nodes alone usually caused a greater magnitude of loss to the connectivity of the network. If we assume the road networks under the disruptions of random diffusive failures as group 1, road networks under the targeted diffusive failures (failures originate from those nodes which are considered significant, i.e. high degree centrality, high betweenness, nodes with low closeness centrality and nodes with high Eigenvector centrality) as group 2. Overall connectivities of the network in these two groups have been studied. OC values for each of the 88 super neighborhoods are studied.

### III. CASE STUDY RESULTS AND DISCUSSIONS

- **Road Network and Hydraulic Process**

This study demonstrated the estimation of the parameters of the SIS model using the road network in Memorial Super Neighborhood (SN-16), which is located on the west side of Houston and one of those areas suffered heavily from road closures chiefly due to fluvial flooding during Hurricane Harvey. This road network has 4073 nodes and more than 9785 edges, with an average node degree of 2.398. As a proxy for the flood vulnerability, the elevation of each node in the network was also retrieved using Google API. Data for the road network was obtained from OpenStreetMap using the OSMnx python package (Boeing, 2017). During Harvey, flooding in the study started at 20:00:00 on August 26, 2017. The temporal changes in the flood depth at the node location in the road network is obtained for a temporal scale of 17 days, observations are in hourly intervals, from 12 AM, 25 August 2017 to 11 PM, 10 September 2017. A snapshot of the road network when the most severe flooding occurred can be seen from Figure 4, which happened at 11:00:00 on August 30<sup>th</sup>, 2017, when the maximum number of nodes (937 nodes out of 4073) flooded in the network. This study looked into the time between 22:00:00 on August 26, 2017, and above peak period, which is 11:00:00 on August 30, 2017. A temporal change in the fraction of flooded nodes (as long as a node is under non-zero flood water, it was considered as flooded) can be seen from below Figure 4. As can be seen from Figure 5, using the size of the giant component in the network, resilience triangles were obtained for the road network under different node-removal criteria (which corresponds to road closure to different types of vehicles).

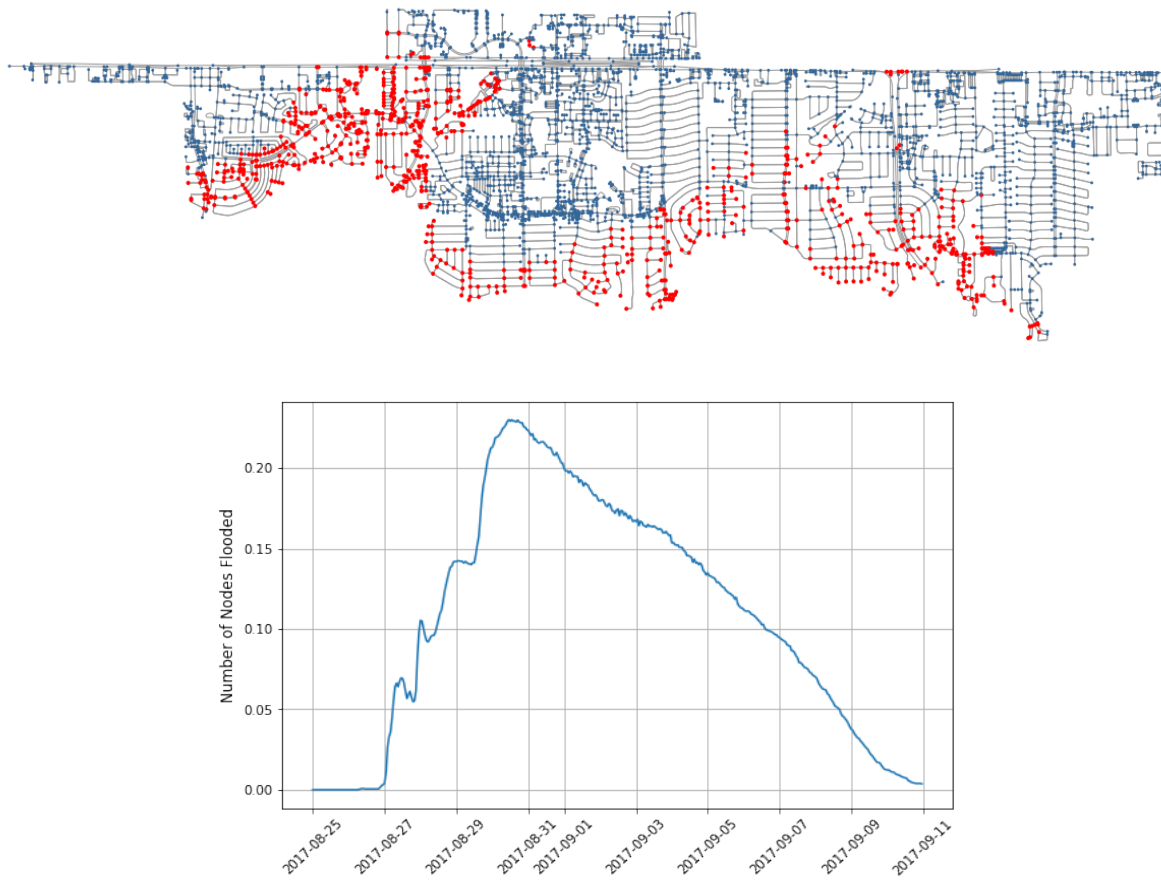


**Figure 4 Road Network under Maximum Flooding (top); Temporal Change in the Number of Inundated Nodes in the Road Network (bottom)**

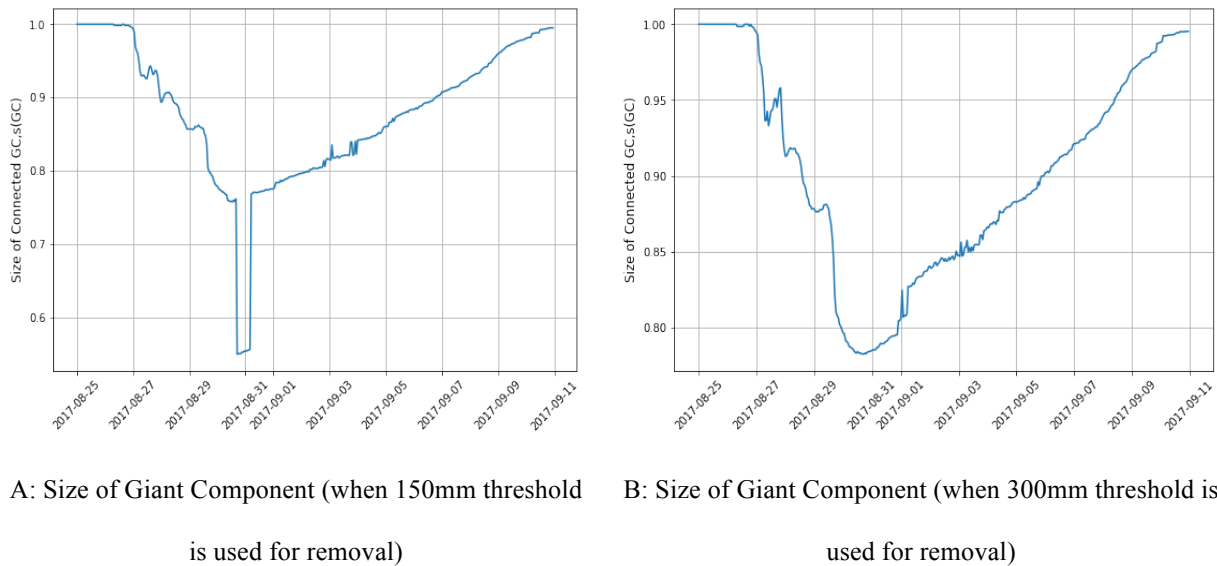


**Figure 5 Sizes of GC in Road Network under Two Different Closure Thresholds**

- **Obtaining the Network Diffusion Parameters**

Three parameters, as discussed in the methodology section, needed to be estimated for an SIS diffusion model. The initially impacted parameter was estimated based on the number of nodes within a certain type of flood plain. The transition rate parameters ( $\beta$  and  $\gamma$ ) were estimated by minimizing residual sum of squares method. In other words, the sum of squares of the difference between predicted and observed node numbers in each category is minimized. **Table 1** presents a summary of the parameter estimation for the SIS model under four different flood threshold scenarios. These four scenarios are considered because these values represent the threshold values for the propagation of flood-induced road closure in the road network for different types of vehicles. As discussed in methodology section, 150mm represents the maximum flood depth in which sedan cars can travel on the road while 300 mm represents the depth for SUV vehicles, whereas 600mm represents the threshold flood depth for the fire trucks. The 0mm shows the results when the threshold value for the flood is binary, as long as there is a flood on the location where nodes lie, the node is considered flooding.

**Table 1 Summary of Diffusion Parameters under Different Diffusion Threshold**

| Diffusion Threshold (in mm) | Beta ( $\beta$ ) | Gamma ( $\gamma$ ) | Initially Impacted (% of nodes) |
|-----------------------------|------------------|--------------------|---------------------------------|
| 0                           | 0.025            | 0.02               | 1                               |
| 150                         | 0.02             | 0.013              | 0.8                             |
| 300                         | 0.03             | 0.024              | 0.5                             |
| 600                         | 0.02             | 0.015              | 0.4                             |

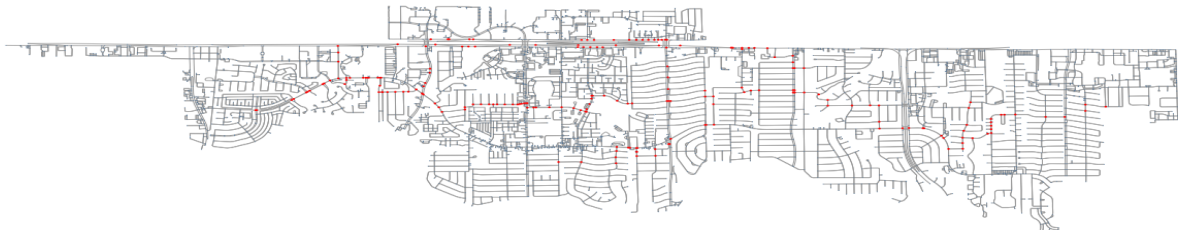
- **Experiment One: Assessing the Impact of Diffusion on Connectivity Profile**

This study first estimated the parameters of the SIS diffusion based on the actual hydraulic process in the road network, which facilitated simulations of the road network diffusion under various hypothetical fluvial flooding events. A better understanding of the impact of parameters of the SIS diffusion model on the diffusion profile of the road networks is crucial as different combinations of  $\beta$  and

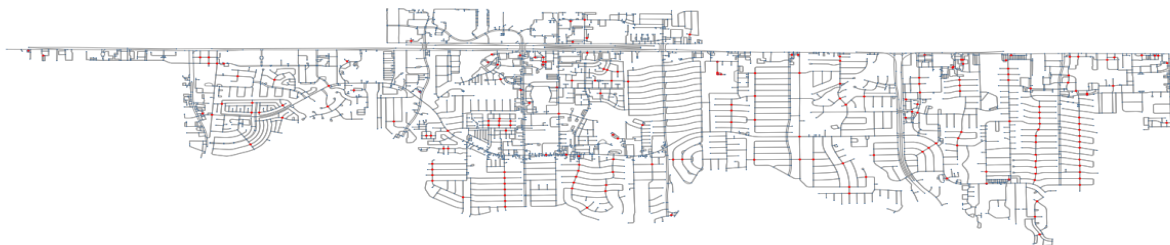
$\gamma$  values represent a different flooding profile, like the intensity of precipitation, runoff, the capacity of the flood control infrastructure or drainage systems. Furthermore, once an estimate of the values for the SIS diffusion parameters, Beta ( $\beta$ ) and Gamma ( $\gamma$ ), are obtained, it is possible to conduct scenario analysis by initiating the diffusion from different locations in the road network, which represents areas fluvial flooding most likely starts. The diffusion which starts from randomly selected seed nodes is a baseline scenario in which the flood originates in the road network from a set of randomly chosen nodes. Figure 6 (highlighted in red) shows a set of randomly chosen nodes that serve as the seed nodes for the diffusion. In order to facilitate a comparison between different scenarios, 5% of the total node number were selected for all the scenarios and diffusions are simulated in the same network in Memorial Super Neighborhood.



A: Randomly Chosen Seeds



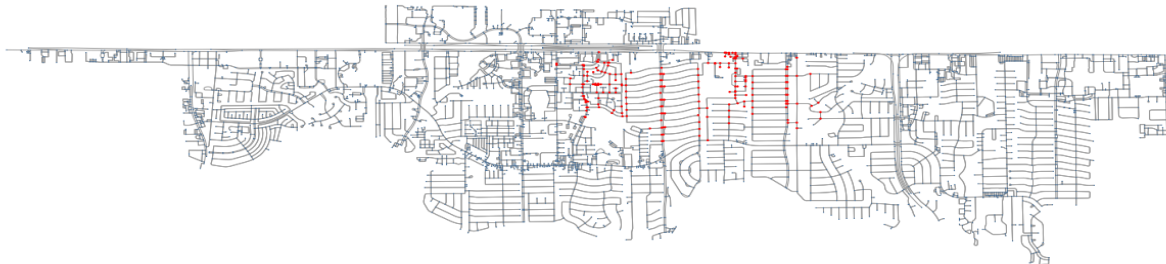
B: High Betweenness Centrality Seeds



C: High Degree Centrality Seeds



D: High Eigen Value Centrality Seeds



E: High Closeness Centrality Seeds

**Figure 6 Locations of Seed Nodes in Road Network**

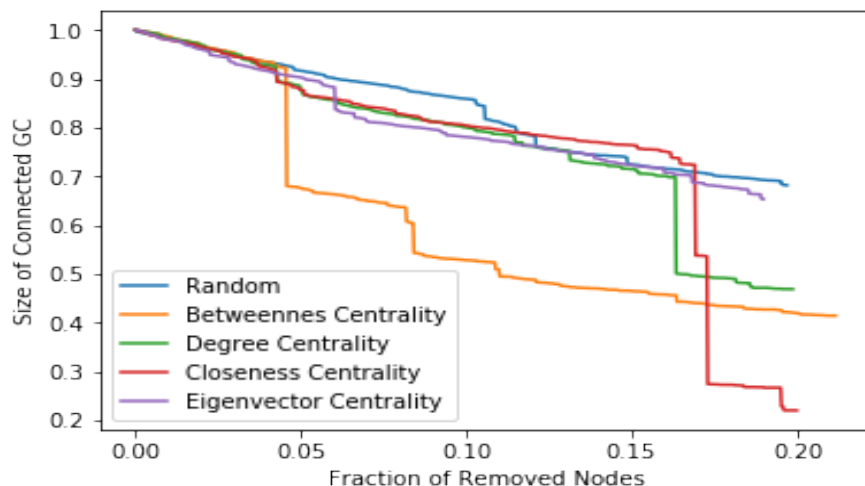


**Figure 7 Diffusion Profile of Road Network under Different Seed Locations**

As could be seen from Figure 7, the rate at which the connectivity of the road network is reduced under different diffusion scenarios varies significantly. There is an apparent non-linear pattern of reduction in the connectivity of road networks when diffusion in the road network is initiated from nodes with high betweenness, degree and closeness centralities. At different magnitudes of disruption (as the

fraction of removed nodes varies in x-axis), the overall reduction of the connectivity of the road network is also different.

- **Experiment Two: Characterization of Road Network Vulnerability to Diffusive Disruptions**

A separate simulation of diffusion on the road network was conducted for each of the scenarios (random, BE, DC, CC, and EC). The working hypothesis is that a diffusion starts from nodes with high centrality values will cause a greater loss in the connectivity. According to this hypothesis, the average connectivity of the road network under these scenarios ( $\mu_{AD}$ ,  $\mu_{BC}$ ,  $\mu_{CC}$ ,  $\mu_{EC}$ ) is less than connectivity of the road network under a diffusive failure which starts from a set of nodes randomly chosen. The parameters of the diffusion are initially impacted seed size  $\alpha$  ( $\alpha = 1\%$ ,  $5\%$  and  $10\%$ ),  $\beta = 0.04$ ;  $\gamma = 0.02$ . This process was conducted for 88 super neighborhoods in Houston, in order to get the sample of the road network connectivity under these scenarios. Independence between samples was assumed, as the number of samples is more than 30, the z-test was used for testing the hypothesis. Table 2 presents a summary of the hypothesis testing when the seed size parameter is  $\alpha = 10\%$ . When larger seed size values ( $1\%$  and  $5\%$ ) are used, the results for tall high centrality scenarios (high DC, EC, CC and BC) centrality scenarios are not significantly different from the diffusion initiated from randomly chosen seeds.

**Table 2 Results of the Hypothesis Tests (on the different networks)**

| Initial Seed Type | Working Hypothesis        | z-statistics | Conclusion (at $\alpha = 0.1$ ) |
|-------------------|---------------------------|--------------|---------------------------------|
| high DC           | $\mu_{AD} < \mu_{random}$ | 0.214921     | Fail to reject the Null         |
| high BC           | $\mu_{BC} < \mu_{random}$ | 2.078136     | Reject the Null                 |
| high CC           | $\mu_{CC} < \mu_{random}$ | 0.677877     | Fail to reject the Null         |
| high EC           | $\mu_{EC} < \mu_{random}$ | 1.780124     | Reject the Null                 |

As could be inferred from the results in Table 2, contrary to the initial belief, diffusion started from high significance nodes do not cause the expected greater decrease in the network connectivity.

Diffusion which originates from seeds of nodes that have high betweenness and high eigenvector centrality causes greater loss to the connectivity loss when the seed size is large, compared to ones that started from randomly selected nodes. In contrast, diffusion which originates from seeds of nodes that have high closeness centrality seems to cause less loss to the connectivity of the network than a diffusion started from the randomly chosen nodes.

Average connectivities in road networks (for the above-mentioned five cases) under different seed-size scenarios were also studied (see Figure 8). Diffusion which originates from seeds of nodes that have high eigenvector and betweenness centrality seems to cause more significant loss to the connectivity loss when the seed sizes are respectively 2% and 4%. It is also observed that if diffusion starts from a larger number of nodes ( above 7% of total nodes) with high betweenness centrality, the impacts on the network connectivity would be higher than that of diffusion originated from the randomly chosen nodes with the same size.

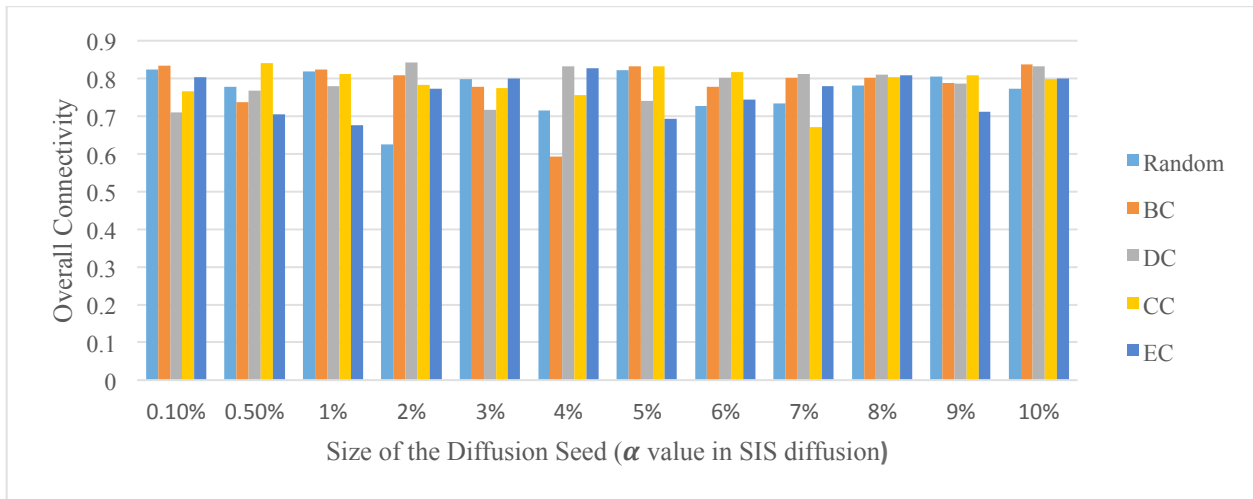


**Figure 8 Average Network Connectivity under different Diffusion Scenarios**

The above findings have important implications for flood management. The figures indicate that to ensure the connectivity of the graph or the transportation network, it is crucial to maintain the functionality of a number of critical nodes in the network. This paper illustrates that the SIS diffusion model can be used to identify critical nodes in transportation road networks. This paper also presented a sensitivity analysis of the impact of the number of initially flooded nodes. The second application of the

finding is that network size increase may not necessarily result in improved robustness in the network. This also means that just adding extra lanes to the roadways may not improve the flood resilience of the road network. Instead, working on ensuring the functionality of a few nodes in road networks is critical to the robustness of the road network.

#### IV. CONCLUSIONS

This paper presented the use of SIS diffusion model used to study the spread of communicable diseases to study diffusion phenomena in the road network under the influence of the fluvial flooding during heavy rainfall. The results show that this model can be used to study the flood vulnerability of road networks. In addition, the results indicate that the road network studied does have critical threshold values for the impacted nodes, being above which could lead to the wholesale closure of the roads networks, which could lead to serious consequences in terms of the social and economic well-being of the people. It has been observed that the sensitivity of the robustness of the road network is different for the random percolation and diffusive network. It has been observed that the rate of the reduction in the robustness is faster under the SIS diffusive phenomenon than in the random percolation. In summary, If we are able to predict the configuration of the road network under a given flooding scenario, then we would be able to predict various types of accessibilities. There is also a threshold value for the node removal portion for the robustness decrease, while the change in the robustness (measured in terms of the largest connected component) under the random percolation is relatively moderate. The critical threshold value for the removal portion of the nodes under the diffusion phenomenon is about 25%. This has two critical implications on the road networks. The first, marginal utility of the investment on improving the vulnerability of the road network is different at different disruption levels, the dividend, in terms of the ensuring the robustness of the network, on investing to ensure the node-removal doesn't exceed the threshold value, which is about 25% is much larger than investing in ensuring, say 15%, of the node removal.

Even though this study has addressed the limitations of the existing literature by treating the condition of the road network (depth of the flooding) as a continuous variable, not as binary variables as closed or functional. This does not mean this study is without limitations. For example, even though the depth of the standing floodwater in the road network is an important indicator for it's being closed or not, in order to render it nonfunctional, there could be numerous other factors like, vehicle conditions (tire pressure, roadworthiness etc.), condition of the pavement, visibility and aptitude and behavior of the driver during the flooding events, which could contribute to the whether a road network is being "closed" or not. In terms of the granularity of the data, this study has used the hourly flood depth data as input for the diffusion. This granularity could lead to some cases where the depth of the flood in specific nodes is zero in one instance and quickly becomes too large to the extent that the node being removed. This process is not captured in the  $S \rightarrow I \rightarrow S$  transition process. It is also possible to train diffusion models using the data for multiple super neighborhoods or under multiple types of flooding scenarios, which could enable the identification of the diffusion model that is best able to model the floodwater diffusion in road networks during a given flooding event.

## V. REFERENCES

Abdulla, B., Mostafavi, A., & Birgisson, B. (2019). Characterization of the Vulnerability of Road Networks to Fluvial Flooding Using Network Percolation Approach. In *Computing in Civil Engineering 2019: Smart Cities, Sustainability, and Resilience* (pp. 428–435). American Society of Civil Engineers Reston, VA.

ASCE. (2017). Report Card for America's Infrastructure. Retrieved May 9, 2019, from <https://www.infrastructurereportcard.org/>

Ashley, S. T., & Ashley, W. S. (2008). Flood fatalities in the United States. *Journal of Applied Meteorology and Climatology*, 47(3), 805–818.

Bashan, A., Berezin, Y., Buldyrev, S. V., & Havlin, S. (2013). The extreme vulnerability of interdependent spatially embedded networks. *Nature Physics*, 9(10), 667.

Blackburn, J. (2017). Living with Houston Flooding.

Boeing, G. (2017). OSMnx: New methods for acquiring, constructing, analyzing, and visualizing complex street networks. *Computers, Environment and Urban Systems*, 65, 126–139.

Courty, L. G., Rico-Ramirez, M. A., & Pedrozo-Acuna, A. (2017). The Significance of Infiltration and Spatial Variability of Rainfall on the Numerical Reproduction of Urban Floods.

Drobot, S. D., Benight, C., & Gruntfest, E. C. (2007). Risk factors for driving into flooded roads. *Environmental Hazards*, 7(3), 227–234.

Dueñas-Osorio, L., Craig, J. I., Goodno, B. J., & Bostrom, A. (2007). Interdependent response of networked systems. *Journal of Infrastructure Systems*, 13(3), 185–194.

FitzGerald, G., Du, W., Jamal, A., Clark, M., & Hou, X. (2010). Flood fatalities in contemporary Australia (1997–2008). *Emergency Medicine Australasia*, 22(2), 180–186.

Haines, Y. Y., & Jiang, P. (2001). Leontief-based model of risk in complex interconnected infrastructures. *Journal of Infrastructure Systems*, 7(1), 1–12.

Heller, M. (2002). Interdependencies in civil infrastructure systems. In *Frontiers of Engineering: Reports on Leading-Edge Engineering from the 2001 NAE Symposium on Frontiers of Engineering* (p. 47). National Academies Press.

Kalantari, Z., Cavalli, M., Cantone, C., Crema, S., & Destouni, G. (2017). Flood probability quantification for road infrastructure: Data-driven spatial-statistical approach and case study applications. *Science of the Total Environment*, 581, 386–398.

Kiaghadi, A., & Rifai, H. S. (2019). Physical, Chemical, and Microbial Quality of Floodwaters in Houston Following Hurricane Harvey. *Environmental Science & Technology*, 53(9), 4832–4840.

Kreibich, H., Piroth, K., Seifert, I., Maiwald, H., Kunert, U., Schwarz, J., ... Thielen, A. H. (2009). Is flow velocity a significant parameter in flood damage modelling?

Lagmay, A. M., Mendoza, J., Cipriano, F., Delmendo, P. A., Lacsamana, M. N., Moises, M. A., ... Santos, L. (2017). Street floods in Metro Manila and possible solutions. *Journal of Environmental Sciences*, 59, 39–47.

Leu, G., Abbass, H., & Curtis, N. (2010). Resilience of ground transportation networks: a case study on Melbourne.

Newman, M. (2010). *Networks: An Introduction*. OUP Oxford. Retrieved from <https://books.google.com/books?id=LrFaU4XCsUoC>

Newman, M. (2018). *Networks*. Oxford university press.

O'Rourke, T. D. (2007). Critical infrastructure, interdependencies, and resilience. *BRIDGE-WASHINGTON-NATIONAL ACADEMY OF ENGINEERING*-, 37(1), 22.

Pregnolato, M., Ford, A., Wilkinson, S. M., & Dawson, R. J. (2017). The impact of flooding on road transport: A depth-disruption function. *Transportation Research Part D: Transport and Environment*, 55, 67–81.

Pyatkova, K., Chen, A. S., Butler, D., Vojinović, Z., & Djordjević, S. (2019). Assessing the knock-on

effects of flooding on road transportation. *Journal of Environmental Management*, 244, 48–60.

Reed, D. A., Kapur, K. C., & Christie, R. D. (2009). Methodology for assessing the resilience of networked infrastructure. *IEEE Systems Journal*, 3(2), 174–180.

Rodin, J. (2014). *The resilience dividend: being strong in a world where things go wrong*. Public Affairs.

Rossetti, G., Milli, L., Rinzivillo, S., Sîrbu, A., Pedreschi, D., & Giannotti, F. (2018). NDlib: a python library to model and analyze diffusion processes over complex networks. *International Journal of Data Science and Analytics*, 5(1), 61–79.

Sadler, J. M., Haselden, N., Mellon, K., Hackel, A., Son, V., Mayfield, J., ... Goodall, J. L. (2017). Impact of sea-level rise on roadway flooding in the Hampton Roads region, Virginia. *Journal of Infrastructure Systems*, 23(4), 5017006.

Shakarian, P., Bhatnagar, A., Aleali, A., Shaabani, E., & Guo, R. (2015). *Diffusion in social networks*. Springer. Retrieved from <https://link.springer.com/content/pdf/10.1007/978-3-319-23105-1.pdf>

Singh, P., Sinha, V. S. P., Vijhani, A., & Pahuja, N. (2018). Vulnerability assessment of urban road network from urban flood. *International Journal of Disaster Risk Reduction*, 28, 237–250.

Tamvakis, P., & Xenidis, Y. (2013). Comparative evaluation of resilience quantification methods for infrastructure systems. *Procedia-Social and Behavioral Sciences*, 74, 339–348.

van Laere, J., Berggren, P., Gustavsson, P., Ibrahim, O., Johansson, B., Larsson, A., ... Wiberg, C. (2017). Challenges for critical infrastructure resilience: cascading effects of payment system disruptions. In *14th International Conference on Information Systems for Crisis Response and Management (ISCRAM2017), Albi, France, May 21-24, 2017* (Vol. 14, pp. 281–292). ISCRAM.